

Effects of intrinsic spontaneous-emission noise on the nonlinear dynamics of an optically injected semiconductor laser

J. B. Gao, S. K. Hwang, and J. M. Liu

Department of Electrical Engineering, University of California at Los Angeles, Los Angeles, California 90095

(Received 13 March 1998)

The effects of intrinsic spontaneous-emission noise on the nonlinear dynamics of an optically injected semiconductor laser is quantitatively studied through a single-mode model. It is found that for periodic motions, the effect of this noise source is to kick phase points off the underlying deterministic limit cycle. When the noise is not too strong so that phase points can stay near the limit cycle, phase points execute Brownian-like motions. When the noise is very strong, or the convergent flow near the attractor is weak, noise instantly kicks phase points away from the attractor to a region where nonlinearity is very strong. Then the diffusional process is slower than a standard Brownian motion. For chaotic motions, the characteristic short-term predictability of chaos is destroyed with an increasing amount of noise. The chaotic motions near the periodic/chaotic boundary, as well as at some locations inside the chaotic region, are more susceptible to noise. This suggests that there may exist fine structures inside the chaotic region. [S1050-2947(99)01302-5]

PACS number(s): 42.55.Px, 05.45.Xt, 42.60.Mi

Nonlinear dynamics in semiconductor lasers is a subject of considerable current research interest [1]. It was predicted [2], and recently confirmed [3], that external optical injection in a semiconductor laser can lead to chaos through a period-doubling route.

There are two types of noise sources in an optically injected semiconductor laser. One is the intrinsic spontaneous-emission noise, and the other is the extrinsic noise in the injection field. The effect of the intrinsic spontaneous-emission noise on the locked states of an optically injected semiconductor laser were studied in [4–6]. Yamamoto, Machida, and Nilsson suggested [7] that features of the optical spectrum can be related back to fundamental intrinsic noise sources of the system. By including spontaneous emission noise with the noise strength, together with other key dynamic parameters, determined experimentally, it was shown [3] that all of the experimentally observed spectral features for the oscillatory and chaotic states of an optically injected semiconductor laser can be recovered by a single-mode injection model. Few attempts, however, have been made to study the quantitative effects of the intrinsic spontaneous-emission noise on the nonlinear dynamics of semiconductor lasers. Conceivably a deep understanding of this issue will be of great value in the effort to harness the nonlinear dynamics of semiconductor lasers for technological applications. Our purpose in this work is to use a method proposed recently [8] to study quantitatively and systematically how the intrinsic spontaneous-emission noise affects the periodic and chaotic motions of the semiconductor laser. With this purpose in mind, we shall take a clean coherent injection field. Experimentally, this condition is approached by injecting a laser with a laser field that has a much narrower linewidth than the injected laser, such as that from a semiconductor laser operated very high above threshold [3,14].

A single-mode model of a semiconductor laser under external optical injection is cast as follows [3]:

$$\frac{da}{dt} = \frac{1}{2} \left[\frac{\gamma_c \gamma_n}{\gamma_s \tilde{J}} \tilde{n} - \gamma_p (2a + a^2) \right] (1 + a) + \xi \gamma_c \cos(\Omega t + \phi) + \mu F_a, \quad (1)$$

$$\frac{d\phi}{dt} = -\frac{b}{2} \left[\frac{\gamma_c \gamma_n}{\gamma_s \tilde{J}} \tilde{n} - \gamma_p (2a + a^2) \right] - \frac{\xi \gamma_c}{1 + a} \sin(\Omega t + \phi) + \frac{\mu F_\phi}{1 + a}, \quad (2)$$

$$\frac{d\tilde{n}}{dt} = -\gamma_s \tilde{n} - \gamma_n (1 + a)^2 \tilde{n} - \gamma_s \tilde{J} (2a + a^2) + \frac{\gamma_s \gamma_p}{\gamma_c} \tilde{J} (2a + a^2) (1 + a)^2. \quad (3)$$

Here, $a = (|A|/|A_0| - 1)$, where A is the field amplitude of the injected laser, and A_0 is the steady-state field amplitude of the laser in the free-running condition. ϕ is the phase difference between A and A_i , where A_i is the amplitude of the injection field. $\tilde{n} = (N/N_0 - 1)$, where N is the carrier density of the injected laser and N_0 is the steady-state carrier density of the laser in the free-running condition. The injection parameter $\xi = \eta |A_i| / (\gamma_c |A_0|)$ is the strength of the injection field received by the injected laser, where η is the coupling rate of the injection field to the injected laser and γ_c is the cavity decay rate. γ_s , γ_n , and γ_p are the spontaneous carrier relaxation rate, differential carrier relaxation rate, and nonlinear carrier relaxation rate, respectively [9]. $\Omega = \omega_i - \omega_o$ is the frequency detuning of the injection field from the free-running frequency of the injected laser. b is the linewidth enhancement factor. $\tilde{J} = (J/e d - \gamma_s N_0) / \gamma_s N_0$ is the injection current parameter, where J is the injection current density, e is the electronic charge, and d is the active layer thickness of the laser. F_a and F_ϕ are the normalized Lange-

vin noise-source terms due to spontaneous emission in the laser: $\langle F_a(t) \rangle = \langle F_\phi(t) \rangle = 0$, $\langle F_a(t) F_\phi(t') \rangle = 0$, and

$$\begin{aligned} \langle F_a(t) F_a(t') \rangle &= \langle F_\phi(t) F_\phi(t') \rangle \\ &= \frac{R_{sp}}{2|A_0|^2} \delta(t-t') = \frac{\beta \gamma_c}{2\Gamma \tilde{J}} \delta(t-t'), \quad (4) \end{aligned}$$

where R_{sp} and β are the rate [10] and fraction of spontaneous emission into the laser mode, respectively, and Γ is the confinement factor of the laser waveguide. Note that a coefficient μ is introduced before F_a and F_ϕ to indicate the variation of the noise strength in different semiconductor lasers. Hence, $\mu=0$ corresponds to (an unrealistic) clean system, while $\mu=1$ corresponds to experimentally determined noise level for a laser under consideration [10].

The laser under this investigation is a SDL model 5301-G1 laser diode which is an index-guided GaAs/Al_xGa_{1-x}As quantum-well laser with a 500- μm cavity. Throughout this paper, we fix the current injection level at $\tilde{J}=2/3$, which corresponds to an injection current level of 40 mA and a free-running output power of 9 mW. At this current level, the corresponding laser parameters are $\gamma_c = 2.4 \times 10^{11} \text{ s}^{-1}$, $\gamma_s = 1.458 \times 10^9 \text{ s}^{-1}$, $\gamma_n = 1.34 \times 10^9 \text{ s}^{-1}$, $\gamma_p = 2.41 \times 10^9 \text{ s}^{-1}$, $b=4$, $R_{sp} = 4.7 \times 10^{18} \text{ V}^2 \text{ m}^{-2} \text{ s}^{-1}$. Meanwhile, the resonance frequency of this laser in the free-running condition is $f_r = 2.93 \text{ GHz}$. All of these parameters were determined experimentally [9].

The dynamics of the laser under consideration has previously been thoroughly mapped as a function of the injection parameter ξ and the detuning frequency Ω [3,14]. There are two separate chaotic regions [3,14] under the operating conditions studied. In this work, we are specifically interested in the situation where the injection field is tuned to the free-running frequency of the injected laser, $\Omega=0$. We then choose some experimentally most interesting injection levels ξ , which correspond to *P1*, simple single-loop limit-cycle oscillation; *P2*, period doubling, double-loop limit-cycle oscillation; chaos; and near their boundaries. The chaotic states studied here belong to one of the two experimentally mapped chaotic regions [3,14].

For each case, a time series $x(t) = [1 + a(t)] \cos \phi(t)$, of length 2×10^4 points, is recorded with a sampling interval $\delta t = 5 \times 10^{-5} \times 2^{-22}$. For convenience, the time series is renormalized to the unit interval [0,1], and is then analyzed by the time delay embedding technique [11]. This is done by constructing vectors of the form $X_i = (x(i), x(i+L), \dots, x[i + (m-1)L])$, with m being the embedding dimension and L the delay time. Based on the feature of our laser system, and our experience with studies on other noisy dynamical systems [8], we choose m to be 8. Then we determine an optimal L by our optimal embedding technique [12]. It is found that $L=5$ works very well for all the different cases we studied.

Let us first study how intrinsic noise affects the chaotic motions of the semiconductor laser. We choose $0.016 \leq \xi \leq 0.04$, where $\xi=0.016$ is near the chaotic/periodic boundary. It is demonstrated [13] that clean chaotic signals can be conveniently studied by calculating the following time dependent exponent $\Lambda(k)$ curves:

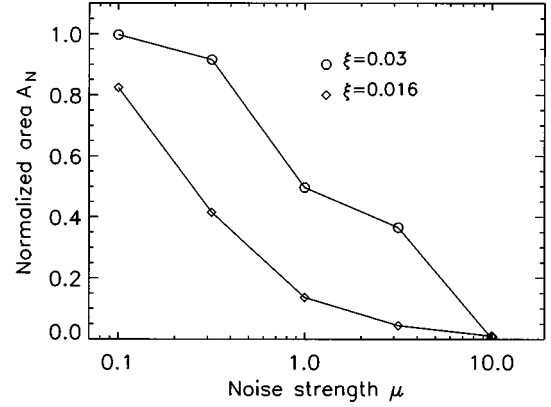


FIG. 1. Variation of the normalized area A_N with normalized noise strength μ for two injection levels $\xi=0.03$ and 0.016 .

$$\Lambda(k) = \left\langle \ln \left(\frac{\|X_{i+k} - X_{j+k}\|}{\|X_i - X_j\|} \right) \right\rangle, \quad (5)$$

with $r \leq \|X_i - X_j\| \leq r + \Delta r$, where r and Δr are prescribed small distances. Geometrically $(r, r + \Delta r)$ defines a shell. The angle brackets denote ensemble averages of all possible pairs of (X_i, X_j) . The integer k corresponds to the evolution time $k \delta t$. For simplicity, we call k the evolution time. The typical shape for $\Lambda(k)$ is that it increases linearly with k till some k_p , then flattens. The linearly increasing parts of the $\Lambda(k)$ curves corresponding to different shells collapse together to form an envelope. This property forms a direct dynamical test for deterministic chaos [13].

For noisy chaotic signals, it is more convenient to work with the logarithmic displacement curves [8]. This is done by rewriting Eq. (5) as

$$\langle \ln \|X_{i+k} - X_{j+k}\| \rangle = \langle \ln \|X_i - X_j\| \rangle + \Lambda(k), \quad (6)$$

and plotting $\langle \ln \|X_{i+k} - X_{j+k}\| \rangle$ as a function of the evolution time k . Now the linearly increasing parts of the curves corresponding to different shells separate, representing the short-term memory of the chaotic system. By adding noise, the separation shrinks, reflecting loss of memory. The stronger the noise is, the more the separation shrinks. This can be quantified by taking the ratio of the separation between the displacement curves for the noisy and clean systems. More concretely, we take two logarithmic displacement curves corresponding to different shells, denote them as D_1 and D_2 , calculate the area between them, do this both for the noisy and the clean systems, and take their ratio. Since this ratio is a normalized area, we denote it by A_N . This procedure can be well approximated by the following formula [8]:

$$A_N \approx \frac{\sum_i (D_1(k_i) - D_2(k_i))|_{\text{with noise}}}{\sum_i (D_1(k_i) - D_2(k_i))|_{\text{without noise}}}, \quad (7)$$

with $k_i > (m-1)L$, $i=1,2,3, \dots$. For a chaotic model system such as the Lorenz attractor, A_N monotonically decreases from 1 to 0 with the strength of noise. This is termed as loss of short-term predictability with increasing amount of noise. A natural question for us to ask is thus whether a similar result is true for the semiconductor laser. This is indeed the case, as is shown in Fig. 1 for $\xi=0.016$ and 0.03 .

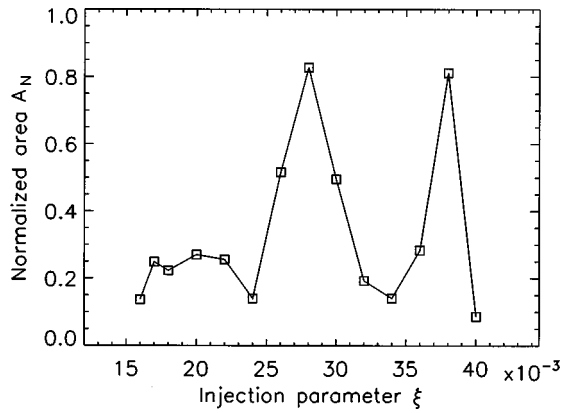


FIG. 2. Variation of the normalized area A_N with injection level ξ for normalized noise strength $\mu=1$.

Figure 1 actually provides us with more information than we have expected. It shows that A_N for $\xi=0.016$ drops much faster than that for $\xi=0.03$. In other words, the chaotic motion for $\xi=0.016$ is much more susceptible to noise than that for $\xi=0.03$. This is reasonable, as one would expect that newly established chaotic motions near the boundary ($\xi=0.016$) between the periodic and chaotic motions is not very stable. This line of reasoning stimulates us to ask an experimentally more important question: In terms of noise susceptibility, what is the variation of A_N with ξ ? Will it be that the chaotic motions near the periodic/chaotic boundaries are all very susceptible to noise, while chaotic motions away from the boundaries are all relatively much less susceptible to noise? To answer this question, we fix the noise to be the experimentally measured level ($\mu=1$), and plot A_N as a function of ξ . Figure 2 shows the result. We observe that there are two large peaks at $\xi=0.028$ and 0.038 , and a local minimum at $\xi=0.034$. This result obviously rejects our simple expectation that the variation of A_N with ξ is relatively simple. Though it does confirm that chaotic states near the boundary are very susceptible to noise, it also suggests that there may exist some fine structures in the chaotic region. Note that there may be several different kinds of fine structures in a chaotic region, depending on one's criteria. For example, for clean chaotic signals, their fractal dimensions and Lyapunov exponents can vary with parameters. These may be regarded as an indication of the existence of a fine structure. However, for noisy chaotic systems, fractal dimensions and Lyapunov exponents are not defined. Hence, this is a much harder issue than that for clean chaotic systems. The criterion adopted in our study is how immune a chaotic system is to an intrinsic noise source. From an experimental point of view, this is a feature that one would be most concerned about.

Next we study how intrinsic noise affects the periodic motions. It has been shown [8] that for the Van der Pol and other oscillators, if the noise is not too strong, then the phase points in the embedding space execute Brownian-like motions near the deterministic limit cycle. Hence the logarithmic displacement curves grow with the evolution time t ($=k\delta t$) very closely as $\ln t^{1/2}$ when t is sufficiently large. Surprisingly this result does not hold here if we use $\mu=1$. An example is shown in Fig. 3 as a group of curves denoted by a . The diamond curve is generated from a curve $\ln t^\alpha$ with $\alpha=0.3$. When we use a smaller noise level ($\mu=0.05^{1/2}$), the

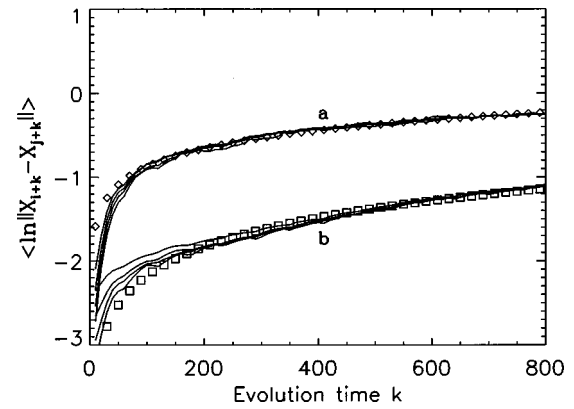


FIG. 3. Four logarithmic displacement $\langle \ln \|X_{i+k} - X_{j+k}\| \rangle$ curves (from top to bottom) corresponding to shells $(2^{-(i+1)/2}, 2^{-i/2})$ with $i=7, 8, 9$, and 10 for $\xi=0.015$. (a) $\mu=1$ and (b) $\mu=0.05^{1/2}$. Also shown in (a) (as diamonds) and (b) (as squares) are curves generated from $\ln t^\alpha$ with $\alpha=0.3$ and 0.5 , respectively.

growth of the logarithmic displacement curves, however, restore to be like $\ln t^{1/2}$. This is shown in Fig. 3 as a group of curves denoted by b . Also shown in curves b is a square curve generated from $\ln t^{1/2}$.

The drop of the exponent α with μ is actually easy to understand. Observe in Fig. 3 that group a curves are way above group b curves. This reflects the fact that in case a the limit cycle is very diffused. In fact, it is so diffused that it is hardly possible to determine by the naked eye where the deterministic limit cycle would locate. It is a reasonably good assumption that the convergent flow near a deterministic limit cycle is constant in an average sense [8], thus producing a Brownian-like motion if the noise is not too strong. However, the validity of this assumption breaks down if the noise is very strong, because the strong noise would kick phase points far off the limit cycle to a region where convergent flow is very nonlinear. Since the system is bounded, the phase points cannot fly too far away. This is why afterwards the diffusional process is slower than a standard Brownian motion, hence a value smaller than 0.5 for the exponent α . Thus we expect that the variation of α with noise strength μ would be that α decreases from $1/2$ to almost zero as μ increases. This is indeed the case, as is shown in Fig. 4 by square and diamond symbols for $\xi=0.01$ and

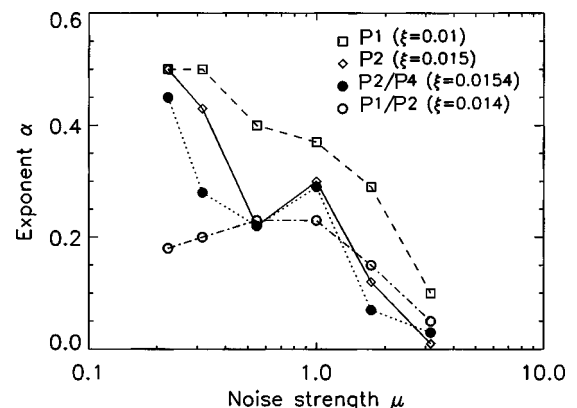


FIG. 4. Variation of the exponent α with normalized noise strength μ for four different injection levels ξ corresponding to four different dynamical states.

0.015, which correspond to $P1$ and $P2$ states, respectively.

This line of argument leads us to expect that the effect of noise would be even more dramatic when ξ is near the bifurcation points, such as the Hopf bifurcation point, $P1/P2$ boundary, or $P2/P4$ boundary, because the convergent flows near the attractors (fixed points or limit cycles) with ξ close to the bifurcation values are very weak. Indeed, if we plot the logarithmic displacement curves for ξ close to the bifurcation values, such as the group a and b curves in Fig. 3, group a curves would be only slightly above group b curves. This is to say that a weak noise already kicks phase points far off the attractor. Further increasing noise only results in kicking the phase points a little bit farther away. This results in a situation where the diffusional process is generally slower than a standard Brownian motion, hence a value smaller than 0.5 for the exponent α . This is shown in Fig. 4 by circle and dark dot curves for $\xi=0.014$ and 0.0154 , which are near the $P1/P2$ and $P2/P4$ boundaries, respectively. A curve similar to that for $\xi=0.014$ is obtained for $\xi=0.006$, which is near the Hopf-bifurcation point.

In summary, for periodic motions, the effects of noise is to kick phase points in the embedding space off the underlying deterministic limit cycle. When the noise is not too strong so that phase points can stay near the limit cycle, such as in the case of $P1$ or $P2$ states, phase points execute Brownian-like motions. When the noise is very strong, or the convergent flow near the attractor is weak, such as in a state near the boundary between $P1$ and $P2$, or $P2$ and $P4$, noise kicks phase points away from the attractor instantly to a re-

gion where nonlinearity is very strong. Afterwards the diffusional process is slower than a standard Brownian motion. For chaotic motions, the characteristic short-term predictability of chaos is destroyed with an increasing amount of noise. The chaotic motions near the periodic/chaotic boundary, as well as at some locations inside the chaotic region, are more susceptible to the noise. This suggests that there exist fine structures inside the chaotic region.

An interesting implication of these results is that when defining concepts such as weak or strong noise, it is better defined by the effects of noise on the nonlinear dynamics, rather than by the noise strength (such as the standard deviation of the noise), as is usually done. For a semiconductor laser, the strength of the spontaneous emission noise to a laser mode depends not only on the structural parameters of the laser but also on the operating point, as can be seen from Eq. (4). Hence, the results from this study imply that the effects of this intrinsic noise on the nonlinear dynamics of a semiconductor laser can vary significantly among lasers of different structural parameters and/or at different operating conditions.

Based on spectral features, two separate chaotic regions were experimentally mapped [3,14] for the optically injected semiconductor laser studied in this paper. In light of current research, we find that the two chaotic regions have to shrink considerably. Some of the originally classified chaotic motions, especially those near the periodic/chaotic boundaries, are actually diffusional processes, not true chaotic motions.

-
- [1] See, for example, *Nonlinear Dynamics in Optical Systems Technical Digest, 1992* (Optical Society of America, Washington, D.C., 1992), Vol. 16; Proc. SPIE **2039** (1994).
- [2] J. Sacher, D. Baums, P. Panknin, W. Elsasser, and E. O. Gobel, Phys. Rev. A **45**, 1893 (1992).
- [3] T. B. Simpson, J. M. Liu, A. Gavrielides, V. Kovanis, and P. M. Alsing, Appl. Phys. Lett. **64**, 3539 (1994); Phys. Rev. A **51**, 4181 (1995); Appl. Phys. Lett. **67**, 2780 (1995).
- [4] P. Spano, S. Piazzolla, and M. Tamburrini, IEEE J. Quantum Electron. **22**, 427 (1986).
- [5] M. R. Surette, D. R. Hjelm, R. Ellingsen, and A. R. Mickelson, IEEE J. Quantum Electron. **29**, 1046 (1993).
- [6] W. A. van der Graaf, A. M. Levine, and D. Lenstra, IEEE J. Quantum Electron. **33**, 434 (1997).
- [7] Y. Yamamoto, S. Machida, and O. Nilsson, Phys. Rev. A **34**, 4025 (1986).
- [8] J. B. Gao, Physica D **106**, 49 (1997).
- [9] T. B. Simpson and J. M. Liu, J. Appl. Phys. **73**, 2587 (1993); J. M. Liu and T. B. Simpson, IEEE Photonics Technol. Lett. **4**, 380 (1993); IEEE J. Quantum Electron. **30**, 957 (1994).
- [10] T. B. Simpson and J. M. Liu, Opt. Commun. **12**, 43 (1994).
- [11] N. H. Packard, J. P. Crutchfield, J. D. Farmer, and R. S. Shaw, Phys. Rev. Lett. **45**, 712 (1980); F. Takens, in *Dynamical Systems and Turbulence, Lecture Notes in Mathematics*, Vol. 898, edited by D. A. Rand and L. S. Young (Springer-Verlag, Berlin, 1981), p. 366.
- [12] J. B. Gao and Z. M. Zheng, Phys. Lett. A **181**, 153 (1993).
- [13] J. B. Gao and Z. M. Zheng, Europhys. Lett. **25** (7), 485 (1994); Phys. Rev. E **49**, 3807 (1994).
- [14] T. B. Simpson, J. M. Liu, K. F. Huang, and K. Tai, Quantum Semiclass. Opt. **9**, 765 (1997).